Spatiotemporal Heterogeneity in the Electrical Activity of Suprachiasmatic Nuclei Neurons and their Response to Photoperiod

T.M. Brown and H.D. Piggins

J Biol Rhythms 2009; 24; 44
DOI: 10.1177/0748730408327918

Spatiotemporal Heterogeneity in the Electrical Activity of Suprachiasmatic Nuclei Neurons and their Response to Photoperiod

T.M. Brown and H.D. Piggins
Faculty of Life Sciences, University of Manchester, Manchester, UK

Abstract The coordinated activity of thousands of cellular oscillators in the suprachiasmatic nuclei (SCN) temporally regulates mammalian physiology to anticipate daily environmental changes across the seasons. The phasing of clock gene expression varies according to anatomical location in the SCN and is thought to encode photoperiodic information. However, it is unclear whether similar variations in phase occur in the electrical activity of SCN neurons, a measure of both intraSCN signaling and clock output. To address this, we recorded single-unit and multiunit activity (SUA/MUA) from dorsal and ventral subregions of the middle level of the rostrocaudal axis of the SCN in coronal brain slices prepared from mice housed under different photoperiods. We demonstrate that under a symmetrical (12 h light:12 h dark) photoperiod, cells in the dorsal SCN are less tightly synchronized than those in the ventral SCN. Comparison of recordings made from mice under short (8 h light:16 h dark) or long (16 h light:8 h dark) photoperiods shows that the phase distribution of ventral, but not dorsal, SCN neurons expands with increasing day length. Conversely, the duration that individual neurons are active increases in dorsal, but not ventral, SCN under long days. These data indicate that in the ventral SCN photoperiod is encoded at the network level, while this coding occurs at the level of individual cells in the dorsal SCN.

Key words hypothalamus, mouse, electrophysiology, in vitro, seasonal, circadian

Variations in environmental illumination greatly influence mammalian physiology and behavior and the accurate encoding of this photic sensory information is a key task for the nervous system. Such a role is evident in the master circadian pacemaker of the suprachiasmatic nuclei (SCN). Here, the interplay between intracellular canonical clock gene feedback/forward loops and intercellular signaling underpins the SCNs' representation of the 24-h day (Reppert and Weaver, 2002; Ko and Takahashi, 2006; Brown and Piggins, 2007). Photic information communicated directly to the SCN via the non-image-forming retinohypothalamic tract (Morin and Allen, 2006) regulates this interaction to reset the SCN circadian clock and synchronize it to the day-night cycle. Consequently, the daily patterns of clock gene expression and neuronal electrical activity in the SCN broadly reflect the solar day duration.

The SCN also encode seasonal information (Meijer et al., 2007; Sumova et al., 2004). Nocturnal rodents change their duration of behavioral activity in proportion to the length of the night while, at the tissue level, the peak in SCN clock gene expression or action

1. To whom all correspondence should be addressed: T.M. Brown, Faculty of Life Sciences, AV Hill Building, University of Manchester, Manchester, M13 9PT UK; e-mail: timothy.brown@manchester.ac.uk.

JOURNAL OF BIOLOGICAL RHYTHMS, Vol. 24 No. 1, February 2009 44-54
DOI: 10.1177/0748730408327918

potential firing frequency broadens with increasing day length (Pittendrigh and Daan, 1976; Messager et al., 2000; Mrugala et al., 2000; Nuesslein-Hildeshiem et al., 2000; Refinetti, 2002; Carr et al., 2003; Schaap et al., 2003; Inagaki et al., 2007; Naito et al., 2008). Based on mathematical models, it is predicted that this broadening of the zenith in gene expression and neuronal activity with day length is attributable to expansion in the phase distribution among SCN neurons rather than alterations in the duration of time that individual cells are active (Rohling et al., 2006a, 2006b). These forecasts are broadly supported by changes in the profile of SCN multiunit activity of mice under differing photoperiods (VanderLeest et al., 2007); but, surprisingly, the circadian firing patterns of individual neurons discriminated from these recordings do not show changes in either activity duration or phase distribution.

In this study, we used a sensitive electrophysiological recording technique that enables single-unit activity (SUA) in the mouse SCN to be reliably discriminated from in vitro multiunit (MUA) recordings to determine whether only a subpopulation of SCN neurons are involved in photoperiodic coding or if different populations use different mechanisms to represent day length. On the coronal plane, the mouse SCN is anatomically largest at the middle level of the rostrocaudal axis, with a "ventral" subregion containing many neurons that synthesize vasoactive intestinal polypeptide (VIP) and a "dorsal" subregion in which VIP neurons are scarce or absent. We selected this plane of SCN because, at this level of the rostrocaudal axis, 2 electrodes can be visually guided and accurately placed with 1 electrode in the dorsal and 1 in the ventral subregion, thereby enabling SCN electrical activity to be simultaneously assessed in 2 anatomically distinct populations. We tested how neurons in these regions encode day length by recording SUA/MUA in SCN brain slices from mice under symmetrical (12 h:12 h light-dark [LD]), short (8 h:16 h), or long (16 h:8 h) days. We reveal that the distribution of peak phases of neuronal activity in the dorsal SCN does not change as a function of day length, but that the duration individual cells are active expands as day length increases. By contrast, ventral SCN neurons do not exhibit such changes in electrical activity, but do broaden their distribution of peak firing time with longer days. Thus, we establish for the first time, spatiotemporal heterogeneity in the electrical activity of SCN neurons and their responses to photoperiod. Since different populations of SCN neurons project to different brain sites, a key implication of these findings is that downstream target sites can be differentially altered by photoperiod.

MATERIALS AND METHODS

Animals

Adult male C57BL6/j mice (Harlan, Bicester, UK) were group housed under 8 h:16 h, 12 h:12 h, or 16 h:8 h light-dark cycles, at an ambient temperature of 22 ± 1 °C. Food and water were available ad libitum. Zeitgeber time (ZT) 12 was designated as the time of lights-off. For 12 h:12 h LD experiments, animals were maintained under these conditions for >2 weeks prior to experimental procedures. For photoperiod studies mice were maintained under short or long photoperiods for >8 weeks prior to experimentation. Alongside the group housed animals, for both conditions, 2 mice were housed individually in cages equipped with running wheels, to verify the photoperiod was producing the well-established effects on behavior. All scientific procedures were carried out in accordance with the UK Animal (Scientific Procedures) Act 1986.

Slice Preparation

Slices were generally prepared 1 to 2 h after the start of the photophase. For short-day animals, 3 of 7 slices were prepared 1 to 2 h before the end of the photophase MUA peaks in these slices occurred at a similar ZT to those prepared during the early day (9.1 ± 1.9 vs. 8.5 ± 1.2). Mice were killed by cervical dislocation and decapitation, and the brain was placed in 4 °C artificial cerebrospinal fluid (aCSF; pH 7.4) of composition (in mM): NaCl 124, KCl 2.2, KH_2PO4 1.2, $CaCl_2$ 2.5, $MgSO_4$ 1.0, $NaHCO_3$ 25.5, D-glucose 10, and ascorbic acid 1.14. Coronal brain sections (350 μm thick) were cut using a vibroslicer (Campden Instruments, Leicester, UK). An initial slice made at the rostral tip of the optic chiasm (containing ~150 μm of the rostral SCN) was discarded and the subsequent slice (corresponding to ~150 to 500 μm across the mid-rostrocaudal extent of the SCN) was transferred to a brain slice chamber (PDMI-2; Warner Instruments, Hamden, CT) continuously perfused (~1.5 mL/min) with oxygenated (95% O_2/5% CO_2) aCSF supplemented with 0.0005% gentamicin (Sigma, Poole, UK) and warmed to 35 ± 1 °C. In all cases 1 SCN slice was used per animal.

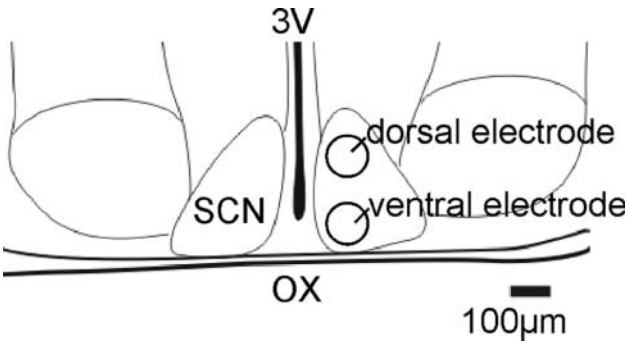

Figure 1. Position of recording sites in mouse suprachiasmatic nuclei (SCN) slices. Schematic diagram of the mouse SCN indicating the locations of dorsal and ventral recording electrodes. Slices contained the mid 350 μm of SCN along the rostrocaudal axis, and at this level, 2 electrodes (tip outer diameter = ~100 μm) could be easily guided to dorsal and ventral positions within the SCN with the aid of a dissecting microscope. Diagram adapted from Paxinos and Franklin (2001).

Electrophysiological Recordings

Extracellular MUA was recorded simultaneously from 2 aCSF-filled suction electrodes constructed as previously described (Brown et al., 2006) and placed unilaterally over dorsal and ventral subregions of 1 SCN (Fig. 1). The SCN multiunit signal was differentially amplified (×20,000) and bandpass filtered (300-3000 Hz) via a Neurolog system (Digitimer, Welwyn Garden City, UK), digitized (25,000 Hz) using a micro 1401 mkII interface (Cambridge Electronic Design [CED], Cambridge, UK), and recorded on a PC running Spike2 version 6 software (CED).

Data Analysis

The total neural activity recorded with a signal to noise ratio of greater than 2:1 is reported as MUA (Hz). As reported, we estimate that these MUA recordings represent the activity of ~10 SCN neurons (Brown et al., 2006). SUA was discriminated from these recordings offline using Spike2 software on the basis of action potential shape and validated by measurement based clustering and the presence of a clear refractory period in an interspike interval histogram (Brown et al., 2005, 2006). Using these criteria we were able to successfully isolate 1 to 4 single units from each MUA recording (mean ± SEM = 2.2 ± 0.1). Period and peak time of SUA and MUA rhythms were determined by curve-fitting using Clockwise software (Bechtold et al., 2008). Strength of clustering in peak times was assessed using Rayleigh plots and phase distributions were compared using Browne-Forsythe's and Levene's tests for equality of variance. Peak widths were assessed over the 1st 24 h in vitro, as the duration of that firing rate was >50% of the maximum values in that epoch; a similar measure has been used previously to characterize the time scales over which SCN cells or populations are active (Schaap et al., 2003; Brown et al., 2006; VanderLeest et al., 2007). Unless otherwise stated, data are presented as mean ± standard error (SEM). Firing rate traces were moderately smoothed using a 1-h running average. Modeling studies and statistical tests were performed using MATLAB R2007a (The Mathworks, Natick, MA).

RESULTS

To test whether neuronal populations in the dorsal and ventral SCN differ in their spontaneous activity patterns, we recorded MUA simultaneously from these 2 subregions of the middle level of the rostrocaudal axis of the SCN (for >48 h) in 16 brain slices from mice housed under a symmetrical 12 h:12 h LD. All MUA recordings exhibited clear circadian rhythms (Fig. 2) and we did not observe any significant difference in the estimated period between recordings from dorsal (23.8 ± 0.3 h) and ventral SCN (23.7 ± 0.2 h; paired t test, $p > 0.05$) or in the breadth of the MUA peak (Fig. 2C; paired t test, $p > 0.05$). In contrast, we did observe a difference in the timing of MUA rhythms with the dorsal SCN consistently peaking later (3.6 ± 1.1 h) in the day than the ventral SCN (Fig. 2B; Wilcoxon matched pairs, $p < 0.05$).

To determine how these observed MUA patterns reflected the activity of individual SCN neurons in dorsal and ventral SCN, we used spike sorting techniques and successfully discriminated 71 cells (Table 1). One dorsal cell and 1 ventral cell exhibited no evidence of circadian rhythmicity and were excluded from further analysis, while the remainder displayed overt ~24-h oscillations (Fig. 3; estimated period dorsal = 23.7 ± 0.4 h, ventral = 23.8 ± 0.4 h; t test, $p > 0.05$). Interestingly, there was a clear difference in the timing of these single-cell rhythms with ventral SCN cells consistently peaking around the mid-projected day, while some dorsal SCN cells peaked during the projected night. Indeed, dorsal SCN cells exhibited a significantly broader distribution in the timing of peak firing than ventral cells (Levene's and Browne-Forsythe's tests, $p < 0.05$), consistent with the weaker clustering in Rayleigh plots of these data (Fig. 3 C, D). In contrast, widths of single-unit peaks and peak firing rates did not differ between

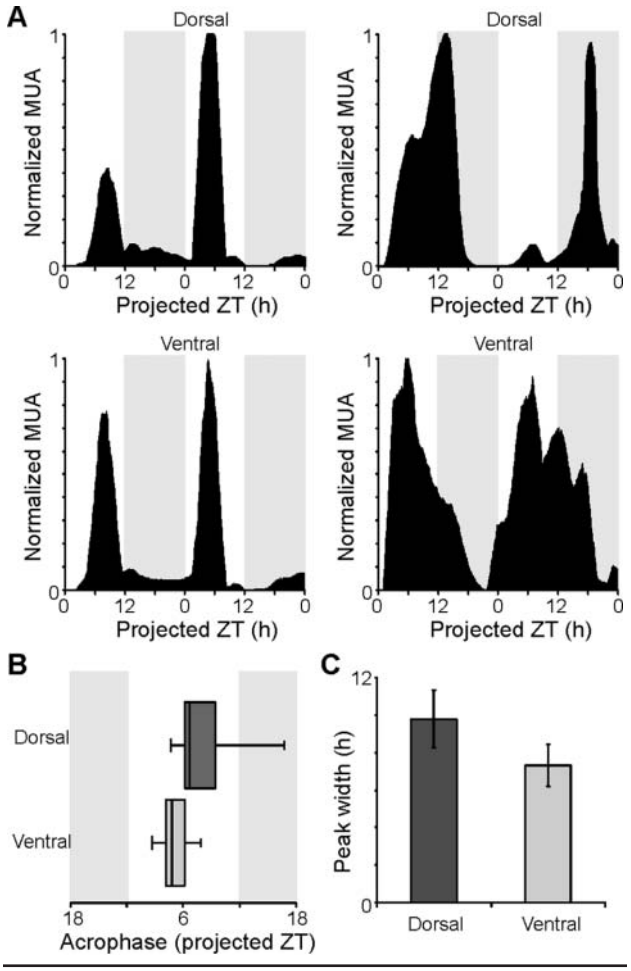

Figure 2. Spontaneous firing rhythms peak later in the dorsal than ventral suprachiasmatic nuclei (SCN). Two examples of multiunit activity (MUA) rhythms (A) recorded simultaneously from dorsal (top) and ventral (bottom) SCN; while ventral SCN MUA consistently peaked during the middle of the projected day, dorsal SCN MUA peaks were more variable in timing and in most cases (15 of 16) peaked later than in the ventral subregion. Peak times of all experiments are shown in B, boxes show 1-3 quartile range, central bar shows median phase, and whiskers show earliest and latest phase. Peak widths (firing duration = >50% max) did not differ between dorsal and ventral SCN (paired *t* test, $p > 0.05$). Firing rate traces in A represent mean firing each minute, moderately smoothed with a 1-h moving average; shaded areas represent projected night phase. Error bars in C indicate SEM.

dorsal and ventral cells (Table 1; *t* tests, $p > 0.05$) and were consistent with values previously reported for rodent SCN neurons in general (Cutler et al., 2003; Schaap et al., 2003; Brown et al., 2006; VanderLeest et al., 2007). Further, we did not observe overt differences in these parameters between day and night peaking cells (data not shown). In summary, these data demonstrate differences in the timing of SUA rhythms between these dorsal and ventral subregions (possibly reflecting differing functional roles) and the absence of difference in the strength of rhythmicity between the 2 neuronal populations.

As discussed above, current models suggest that the SCN encode photoperiod through a broadening of the distribution of peak firing times of individual SCN cells rather than the duration that each cell is active, but available data for single-cell firing patterns support neither this view nor the alternative (VanderLeest et al., 2007). To test whether only a subset of SCN neurons encode photoperiod or if different populations code day length by different mechanisms, we recorded dorsal and ventral SCN MUA for >28 h in slices from 7 mice housed under short days and 8 mice housed under long days (Fig. 4, Table 1). Interestingly, while SCN MUA rhythms recorded from the ventral SCN had significantly broader peak widths under long compared with short photoperiods (Fig. 4D; Table 1; *t* test, $p < 0.05$), dorsal SCN MUA did not (Fig. 4C; Table 1; *t* test, $p > 0.05$). Under both photoperiods, ventral MUA peak times occurred around the middle of the projected day (Fig. 4E, F). Consistent with SCN recordings from the symmetrical 12 h:12 h LD, on average MUA in the dorsal SCN peaked later than ventral MUA under long and short photoperiods (2.3 and 1.3 h later, respectively), although on a within-slice basis these differences were not significant (Fig. 4E, F; Table 1; dorsal later in 6 of 8 long-day and 4 of 7 short-day slices; Wilcoxon matched pairs, $p > 0.05$).

Subsequently, we discriminated the firing patterns of individual SCN neurons contributing to these MUA recordings. We successfully identified 25 cells from our short-day recordings (Fig. 5, Table 1; excluding 1 dorsal cell that did not display a clearly identifiable peak) and 40 cells from our long-day recordings (excluding 1 dorsal and 1 ventral cell that lacked overt rhythmicity). Concordant with our MUA recordings, dorsal cells maintained a broad distribution of peak firing times that did not alter according to photoperiod (Fig. 5A and B, E and F; Levene's and Browne Forsythe's tests, $p > 0.05$), whereas that of ventral cells was broader under long days than 8 h:16 h or 12 h:12 h photoperiods (Fig. 5C and D, G and H; Table 1; Levene's and Browne-Forsythe's tests, $p < 0.05$). Also consistent with our MUA data, the timing of peak firing of dorsal and ventral cells did not show a clear difference under short or long photoperiods (Table 1; Mann-Whitney *U* test, $p > 0.05$). Conversely, analysis of the peak widths and firing rates of SCN

Table 1. Comparison of multiunit and single-unit electrical activity profiles.

		MUA				*SUA*				
		ZT of peak				*ZT of peak*				
	L:D	*Mean*	*SD*	*Peak Width (h: Mean ± SEM)*	n	*Mean*	*SD*	*Peak Width (h: Mean ± SEM)*	*Peak Firing (Hz: Mean ± SEM)*	n
Dorsal SCN	8:16	9.8^{ns}	3.1	8.4 ± 1.4^{ns}	7	11.0^{ns}	4.2^{ns}	4.0 ± 0.5^{b}	2.2 ± 0.4^{b}	12
	12:12	8.7^{a}	4.1	9.8 ± 1.5^{ns}	16	9.7^{a}	5.5^{ns}	4.0 ± 0.4^{b}	2.3 ± 0.3^{b}	35
	16:8	6.4^{ns}	2.3	10.8 ± 0.9^{ns}	8	6.9^{ns}	4.1	5.6 ± 0.5	1.2 ± 0.1	23
Ventral SCN	8:16	8.5	2.8	5.8 ± 1.2^{b}	7	9.3	2.2^{b}	4.0 ± 0.5^{ns}	3.0 ± 0.8^{ns}	12
	12:12	5.1	1.4	7.3 ± 1.1^{ns}	16	5.1	1.9^{b}	3.6 ± 0.4^{ns}	2.7 ± 0.5^{ns}	34
	16:8	4.1	3.9	9.5 ± 1.6	8	7.4	4.0	4.6 ± 0.7	2.0 ± 0.2	15
Pooled	8:16	9.2	2.9	7.1 ± 0.9^{b}	14	10.1	3.4^{ns}	4.0 ± 0.4^{ns}	2.6 ± 0.4^{b}	24
	12:12	6.9	3.5	8.6 ± 1.0^{ns}	32	8.6	4.7^{ns}	3.8 ± 0.3^{ns}	2.6 ± 0.3^{b}	69
	16:8	5.2	3.3	10.6 ± 1.0	16	7.1	4.0	5.1 ± 0.5	1.6 ± 0.1	38

NOTE: The mean ZT of peak firing was compared between dorsal and ventral SCN for each photoperiod by Wilcoxon matched pairs (MUA) or Mann-Whitney *U* test (SUA). Other parameters were compared between long (LD 16:8) and symmetrical (12:12) or short (8:16) photoperiods within each subregion (dorsal, ventral, or pooled) independently. Peak widths and peak firing rates were compared by unpaired *t* test, and the distribution of peak times were compared by Levene's and Browne-Forsythe's tests. SCN = suprachiasmatic nuclei; MUA = multiunit activity; SUA = single-unit activity.
a. Denotes a significant difference within photoperiods ($p < 0.05$) with Wilcoxon matched pairs or Mann-Whitney *U* test.
b. Denotes a significant difference between photoperiods ($p < 0.05$) with *t* test or Levene's and Browne-Forsythe's tests.
ns = $p > 0.05$.

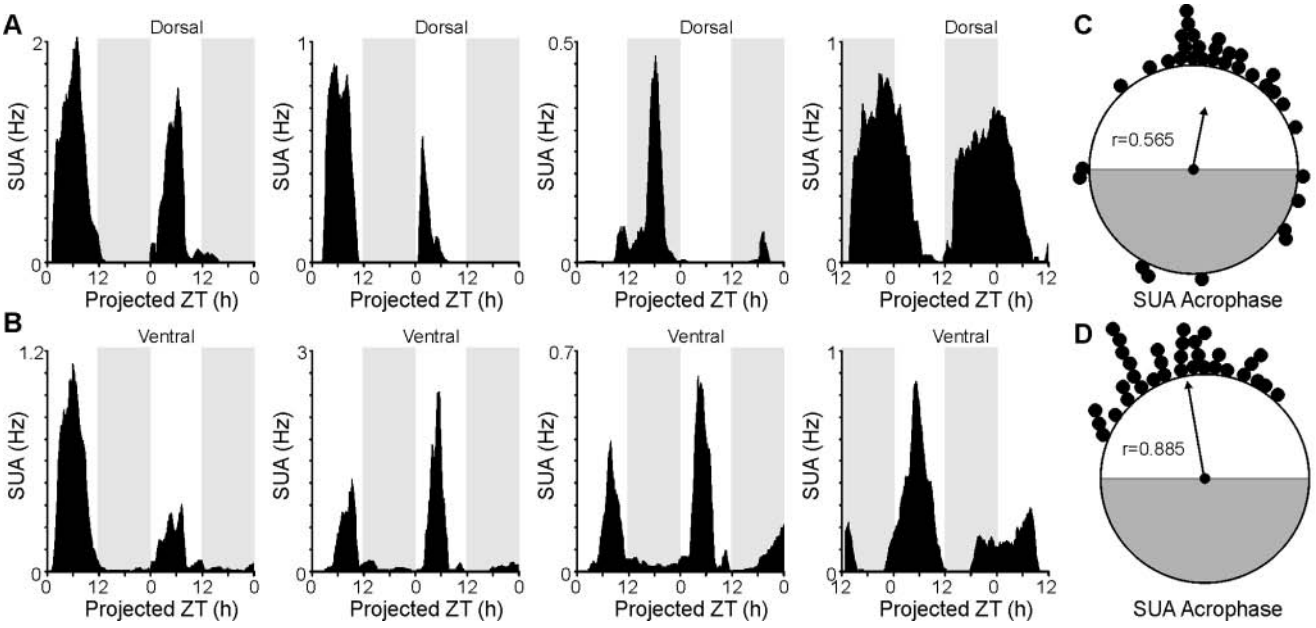

Figure 3. Dorsal suprachiasmatic nuclei (SCN) neurons exhibit a broader range of phasing than ventral cells. Four examples of single-unit activity (SUA) recorded in the dorsal (A) and ventral (B) SCN. Ventral cells consistently displayed peak firing during the projected day phase, while some dorsal cells expressed their peak spiking activity during the projected night. Rayleigh plots of data from all dorsal (C) and ventral (D) cells demonstrate stronger clustering in the peak times of ventral compared with dorsal cells. Firing rate traces in A represent mean firing each minute, moderately smoothed with a 1-h moving average; shaded areas represent the projected night phase. In C and D direction of arrows indicates median phase, length indicates strength of clustering.

neurons demonstrated that dorsal cells displayed significantly broader peak widths and lower firing rates under long, compared with short or symmetrical, photoperiods (Fig. 5I, K; Table 1; *t* tests, $p < 0.05$), while ventral cells did not (Fig. 5J, L; *t* tests, $p > 0.05$). These data demonstrate that SCN subregions recorded in this study encode photoperiod differently, with dorsal neurons changing their daily activity profiles and ventral cells their phase relationships. When data from dorsal and ventral cells were pooled, we

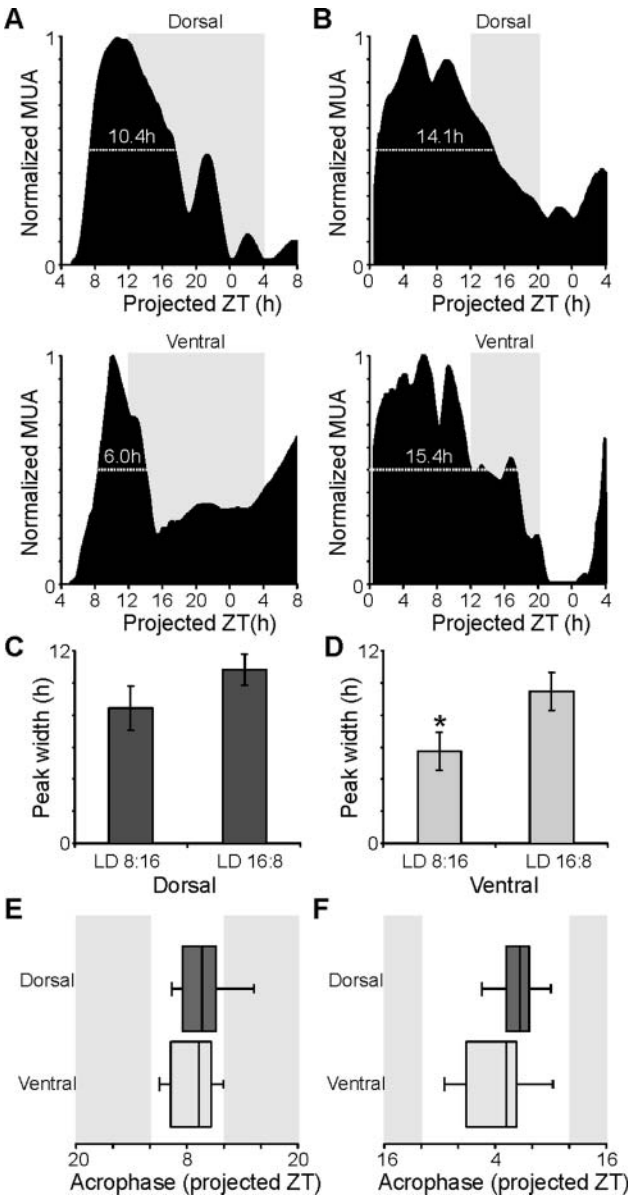

Figure 4. Photoperiod induces more robust changes in ventral rather than dorsal suprachiasmatic nuclei (SCN) multiunit activity (MUA). Examples of MUA recorded simultaneously from dorsal (top) and ventral (bottom) SCN in slices from mice housed under short (A) and long (B) photoperiods. MUA peak widths (firing duration = >50% max) were significantly broader under long days (*t* test, $p < 0.05$) in the ventral (D) but not dorsal (C) SCN (*t* test, $p > 0.05$). Dotted lines on firing rate traces indicate epochs where firing was above 50% of the maximal values and numbers above the lines indicate the calculated peak width. MUA peak times from all short- and long-day photoperiod experiments are summarized in E and F, respectively; boxes show 1-3 quartile range; central bar shows median phase; and whiskers show earliest and latest phase. Firing rate traces in A and B represent mean firing each minute, moderately smoothed with a 1-h moving average; shaded areas represent projected night phase. Error bars in C and D indicate SEM.

did not observe significant changes in either the phase distribution or activity profiles of single cells between short and long days (Table 1; Levene's and Browne-Forsythe's tests and *t* test, respectively, $p < 0.05$). However, consistent with previous work (VanderLeest et al., 2007), the width of MUA peaks was significantly broader in pooled dorsal/ventral data from long compared with short days (Table 1).

Finally, we used the observed single-unit firing patterns to generate average firing rate profiles for single cells from dorsal and ventral SCN under different photoperiods. Using these average profiles and the observed SUA peak times and standard deviations, we modeled the MUA patterns resulting from populations of varying numbers of neurons (Fig. 6). We found that regardless of the size of the neuronal population in the model, changes in the phase distribution of SCN neuronal activity estimated for the ventral SCN (Fig. 6B, D, F) produced a much greater increase in peak width than changes in the width of single-cell waveforms seen in the dorsal SCN (Fig. 6A, C, E).

DISCUSSION

Here, we provide the first demonstration that the phasing and response to photoperiod of electrical rhythms varies within SCN subregions, with ventral cells changing their phase relationships to one another and dorsal cells their activity profiles as a function of day length. Thus, photoperiodic information is encoded in the network activity of ventral SCN neurons but at the level of individual cells in the dorsal SCN. Using a simple mathematical model based on average daily waveforms in electrical activity of SCN neurons recorded in dorsal and ventral portions of the SCN, we show that these changes in single-cell activity are sufficient to account for the alterations in SCN MUA seen in different photoperiods, consistent with previous models (Rohling et al., 2006a, 2006b).

To differentially time changes in physiology in other parts of the brain and body, different populations of SCN neurons should be active at different times of day. Indeed, the existence of such differently phased populations of SCN neurons is inferred from studies on the hypothalamic areas innervated by SCN efferents. Here, inhibitory and excitatory inputs arising from different SCN neurons are implicated in

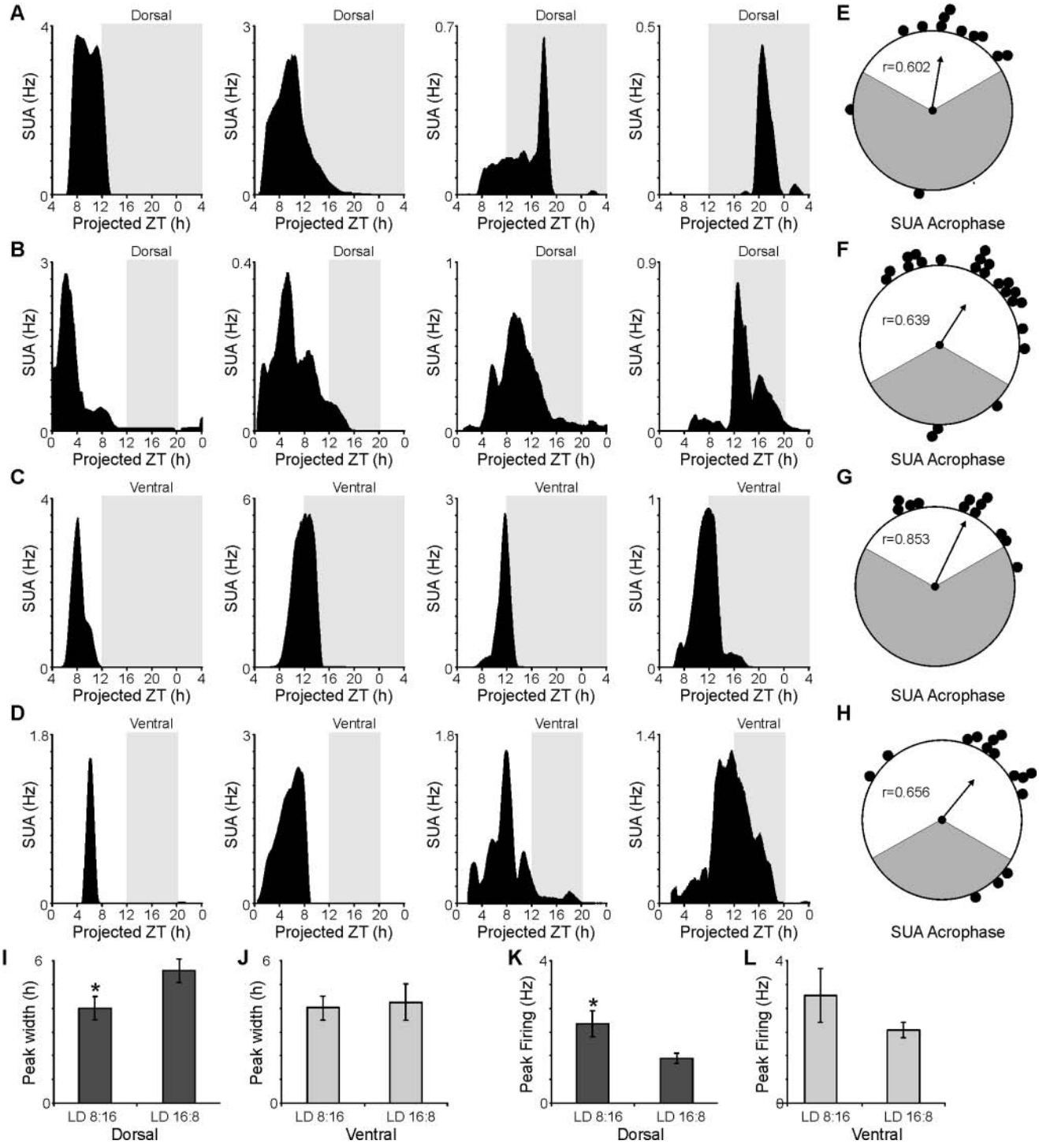

Figure 5. Dorsal and ventral suprachiasmatic nuclei (SCN) neurons respond differently to photoperiod. Four examples of single-unit activity (SUA) recorded in the dorsal (A, B) and ventral (C, D) SCN under short (A, C) and long (B, D) photoperiods. Rayleigh plots of data from all cells indicate that distribution of peak times of dorsal neurons was similar under short (E) and long (F) photoperiods, whereas clustering in ventral cells was stronger under short (G) rather than long (H) days. Conversely, peak widths (duration firing = >50% max) were broader in dorsal SCN cells (I) and firing rates lower (K) under long days (LD 16 h:8 h; *t* tests, $p < 0.05$), whereas peak widths (J) and firing rates (L) in ventral cells did not differ based on photoperiod (*t* tests, $p > 0.05$). Firing rate traces in A to D represent mean firing each minute, moderately smoothed with a 1-h moving average; shaded areas represent projected the night phase. In E and F direction of arrows indicates median phase; length indicates strength of clustering. Error bars in I to L indicate SEM.

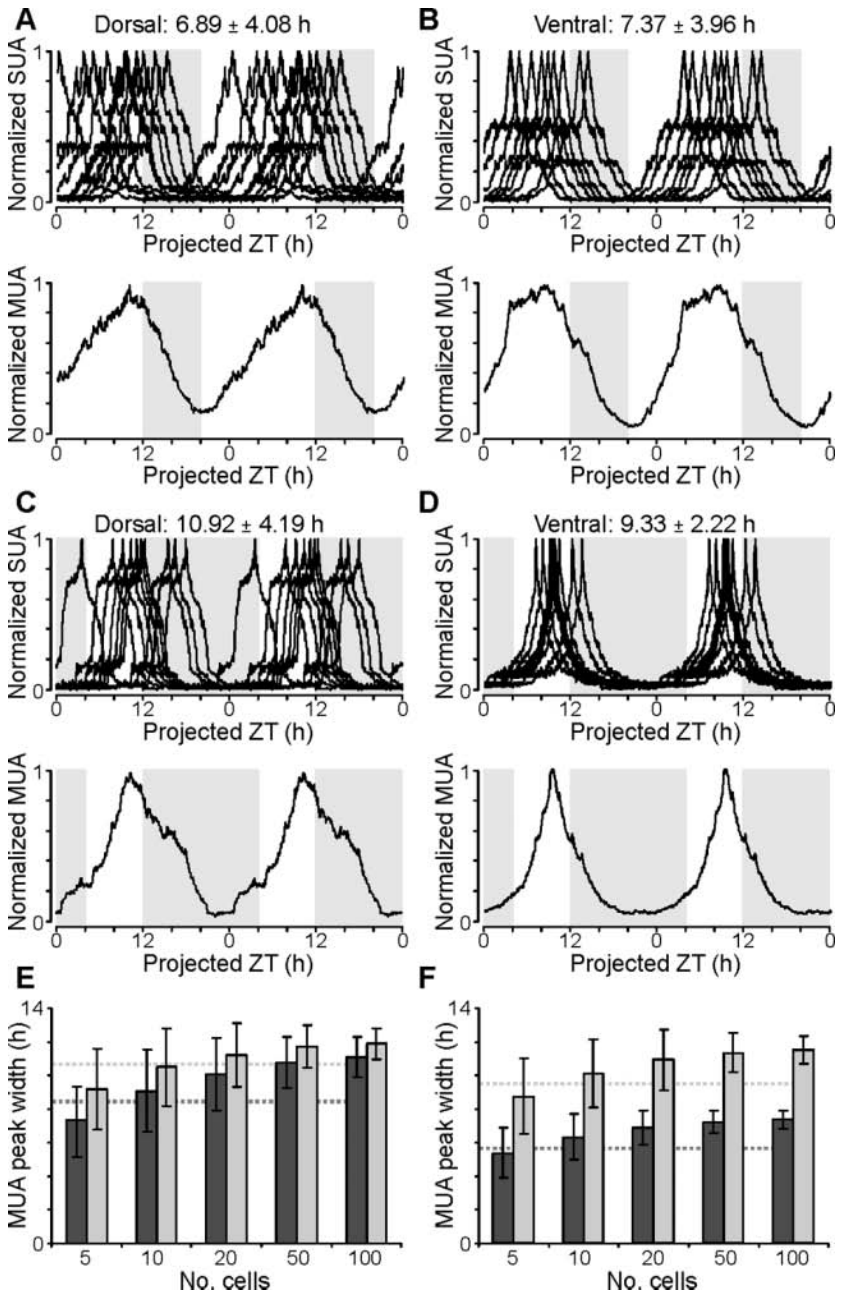

Figure 6. A mathematical model of multiunit firing profiles based on observed single-cell data. We modeled the multiunit activity (MUA) profiles resulting from populations of different numbers of neurons using the average single-cell waveforms normally distributed according to the mean ± SD peak time observed in our experiments. In A to D, top traces show an example population of 10 neurons from dorsal (A, C) and ventral (B, D) suprachiasmatic nuclei (SCN) under short (A, B) and long photoperiods, while bottom traces display the normalized MUA profile resulting from this population. Bar graphs in E and F display the MUA peak widths (±SD) measured from 1000 trials for each condition. Experimentally observed differences in single-unit activities from the dorsal SCN (change in firing rate profile but not phase distribution) could not produce large changes in the MUA peak width (E) between short (dark bars) and long photoperiods (light bars). In contrast, the photoperiod-related differences we observed in ventral SCN cells (change in phase distribution without significant change in individual cells activity profiles) drove a robust increase in peak width under long days. Mean peak widths observed in short- and long-day MUA recordings are represented by lower and upper dotted lines, respectively, and correspond well to the results of the model.

regulating the day-night profile of a diverse range of physiological and behavioral states (Kalsbeek et al., 2006). Thus, our observations that the SCN, as a whole, exhibits a broad range of single-unit firing peak times with several phase groupings fits well into this conceptual framework and is in broad agreement with previous studies imaging *Per1* expression (Quintero et al., 2003; Hughes et al., 2008). Furthermore, since we observed a much broader range of peak times from SCN neurons recorded with our dorsal electrodes, we speculate that cells in this region are better placed to subserve these output functions.

We also demonstrate that ventral and dorsal SCN neurons respond differently to photoperiod. Thus, cells in the ventral SCN alter their distribution of peak times in firing rate proportionally to the length of the light period. However, the durations that these cells are active does not change according to photoperiod and are similar to those reported by VanderLeest et al. (2007). Dorsal SCN cells may also change the timing of their electrical activity rhythms when an animal moves from short to long days, but at the population level, an overall broadening of the phase distribution is not detectable. In this respect, our data for dorsal SCN neurons are consistent with the SUA phase distributions reported by VanderLeest et al. However, we observed a broadening in the daily activity profiles of individual dorsal SCN cells under long days that was not evident in that previous study. Based on demonstrations that ventral SCN neurons appear to entrain cells in the dorsal portion (Yamaguchi et al., 2003; Noguchi et al., 2004; Albus et al., 2005), we

posit that the phase distribution of ventral SCN cells encodes photoperiodic information and that changes in the activity of this population are translated into changes in the duration that individual cells in the dorsal SCN are active. This change in the spiking activity of dorsal SCN neurons then allows this population to regulate activity in their targets over different time scales depending on day length. Alternatively, photoperiodic information may be communicated directly to these dorsal SCN neurons via the retinohypothalamic tract, which is now known to innervate the majority of the mouse SCN (Hattar et al., 2006).

A previous study that did not distinguish between dorsal and ventral SCN found photoperiod-related changes in MUA but not in either SUA phase distributions or activity durations (VanderLeest et al., 2007). Consistent with these findings, when we pooled dorsal and ventral data photoperiod-related differences in the SUA, but not MUA, parameters disappeared. Other recent reports investigated the effects of photoperiod on *Per1*-driven luciferase rhythms in SCN neurons (Inagaki et al., 2007; Naito et al., 2008). These studies demonstrate an overall broadening of phase distribution under long days, consistent with our results, as well as rostrocaudal differences in response to photoperiod. Our preparation (350 μm in the middle of the rostrocaudal axis) presumably includes a mixture of populations designated rostral and caudal in these imaging studies. Importantly, however, Naito et al. (2008) also quantify *Per1* expression between dorsal and ventral portions of the mid-SCN. Although these authors do not report single-cell data, they do show that the population peak broadens considerably more in the ventral compared with dorsal SCN. This is in accord with our experimental data and modeling studies, indicating that the change in ventral SCN SUA can drive a bigger increase in multiunit peak width than changes seen in the dorsal SCN.

In addition to the imaging studies discussed above, other authors have reported gradients of *Per1*-gene expression along various axes (Quintero et al., 2003; Yamaguchi et al., 2003; Hughes et al., 2008). Our data showing earlier peaks in the ventral compared with dorsal SCN under a symmetrical photoperiod are consistent with those of Hughes et al. (2008), but not Yamaguchi and colleagues (2003) who report the opposite relationship. The reasons for this discrepancy are unclear, but it is possible that the SCN network organization in the neonatal slice cultures used in the latter study differs somewhat from the entrained adult SCN used in the present study and by Hughes et al.

Based on initial evidence for a positive correlation between spiking rate and *Per1*-driven GFP expression in SCN neurons (Quintero et al., 2003), it is tempting to interpret the imaging studies discussed above as indirectly reporting SCN neuronal output. However, this correlation was based on recordings performed over a very limited portion of the projected day (ZT 4-7) and the relationship between *Per1* expression and firing rate is more complex than initially reported, varying at different times of the circadian cycle (Belle et al., 2008). In addition, it is likely that some SCN neurons do not express the core molecular clockworks monitored in these imaging studies but may exhibit rhythms in firing frequency driven by other clock cells or inputs to the SCN. For example, previous work demonstrates that light-responsive SCN neurons (as assessed by FOS expression in response to a light pulse) overlap with a population of cells that do not express *period* genes (Karatsoreos et al., 2004). Our data demonstrate that many SCN neurons display electrical rhythmicity (at least over 48 h in vitro), suggesting that cells lacking core components of the molecular clockwork may well exhibit electrical rhythms. Thus, these imaging studies are not necessarily predictive as to how electrical activity varies throughout the SCN under different photoperiods (e.g., Vansteensel et al., 2003). We now provide the first demonstration of dorsal-ventral differences in mid-SCN neuronal output under different entraining conditions. With the predominance of VIP-containing neurons in the ventral subregion of the mid-SCN, it is tempting to speculate that it is these VIP cells that differentially respond to photoperiod. Similarly, in the dorsal subregion of the mid-SCN, neurons expressing arginine vasopressin and somatostatin would be predicted to contribute to these extracellularly recorded electrical signals. However, extracellular recordings such as those used in this investigation do not allow the neurochemical phenotype of the neurons that are the source of the recordings to be identified. Indeed our dorsal/ventral recordings themselves likely represent a mixed population of neurons that may not all respond to photoperiod in the same way. An example of this kind of heterogeneity is seen in the small population of SCN neurons that peak during the projected night. It is currently unclear how the afferent/efferent connectivity and neurochemical phenotype of such cells differs from the majority of (day peaking) SCN neurons. Further work using mice in which the different neuropeptidergic neurons of the SCN or its inputs express different fluorescent constructs is required to satisfactorily determine predictors of SCN neuronal activity under different entrainment conditions.

The utility of ventral/dorsal divisions of the SCN is currently much debated (Morin, 2007), and while they do represent an oversimplification of SCN anatomy/neurochemistry, our data demonstrate that they provide a useful starting point for investigations into SCN function. Thus, we show differences in the timing of electrical activity of cells in the dorsal and ventral SCN and their response to photoperiod that are consistent with existing models of SCN organization and photoperiodic encoding. Moreover, we provide the first evidence that populations of cells in the dorsal and ventral SCN encode day length via different mechanisms. Advances in imaging and electrophysiological recording techniques coupled with cell-type–specific markers will enable refinement of models generated from these simplified anatomical distinctions. In particular approaches that can continuously monitor clock gene expression and electrical activity in phenotypically identified neurons will be invaluable in unraveling the complexities of the SCN clockworks.

ACKNOWLEDGMENTS

We thank Rayna Samuels for her expert technical assistance and Dr. Mino Belle and Professor Robert Lucas for insightful comments on a draft of this article. This work was funded by a project to HDP from the Biotechnology and Biological Science Research Council U.K.

REFERENCES

Albus H, Vansteensel MJ, Michel S, Block GD, and Meijer JH (2005) A GABAergic mechanism is necessary for coupling dissociable ventral and dorsal regional oscillators within the circadian clock. Curr Biol 15:886-893.

Bechtold DA, Brown TM, Luckman SM, and Piggins HD (2008) Metabolic rhythm abnormalities in mice lacking VIP-VPAC2 signaling. Am J Physiol Regul Integr Comp Physiol 294:R344-R351.

Belle MD, Scott F, and Piggins HD (2008) Diurnal and nocturnal temporal silencing of Period1:D2gfp neurons in the suprachiasmatic (SCN) nucleus of mice. Presented at the 20th meeting of the Society for Research on Biological Rhythms, May 17-21, 2008, Destin, Florida.

Brown TM, Hughes AT, and Piggins HD (2005) Gastrin-releasing peptide promotes suprachiasmatic nuclei cellular rhythmicity in the absence of vasoactive intestinal polypeptide-VPAC2 receptor signaling. J Neurosci 25:11155-11164.

Brown TM, Banks JR, and Piggins HD (2006) A novel suction electrode recording technique for monitoring circadian rhythms in single and multiunit discharge from brain slices. J Neurosci Methods 156:173-181.

Brown TM and Piggins HD (2007) Electrophysiology of the suprachiasmatic circadian clock. Prog Neurobiol 82: 229-255.

Carr AJ, Johnston JD, Semikhodskii AG, Nolan T, Cagampang FR, Stirland JA, and Loudon AS (2003) Photoperiod differentially regulates circadian oscillators in central and peripheral tissues of the Syrian hamster. Curr Biol 13:1543-1548.

Cutler DJ, Haraura M, Reed HE, Shen S, Sheward WJ, Morrison CF, Marston HM, Harmar AJ, and Piggins HD (2003) The mouse VPAC2 receptor confers suprachiasmatic nuclei cellular rhythmicity and responsiveness to vasoactive intestinal polypeptide in vitro. Eur J Neurosci 17:197-204.

Hattar S, Kumar M, Park A, Tong P, Tung J, Yau KW, and Berson DM (2006) Central projections of melanopsin-expressing retinal ganglion cells in the mouse. J Comp Neurol 497:326-349.

Hughes AT, Guilding C, Lennox L, Samuels RE, McMahon DG, and Piggins HD (2008) Live imaging of altered period1 expression in the suprachiasmatic nuclei of Vipr2(−/−) mice. J Neurochem 106:1646-1657.

Inagaki N, Honma S, Ono D, Tanahashi Y, and Honma K (2007) Separate oscillating cell groups in mouse suprachiasmatic nucleus couple photoperiodically to the onset and end of daily activity. Proc Natl Acad Sci U S A 104:7664-7669.

Kalsbeek A, Perreau-Lenz S, and Buijs RM (2006) A network of (autonomic) clock outputs. Chronobiol Int 23:521-535.

Karatsoreos IN, Yan L, LeSauter J, and Silver R (2004) Phenotype matters: Identification of light-responsive cells in the mouse suprachiasmatic nucleus. J Neurosci 24:68-75.

Ko CH and Takahashi JS (2006) Molecular components of the mammalian circadian clock. Hum Mol Genet 15:R271-R277.

Meijer JH, Michel S, and Vansteensel MJ (2007) Processing of daily and seasonal light information in the mammalian circadian clock. Gen Comp Endocrinol 152:159-164.

Messager S, Hazlerigg DG, Mercer JG, and Morgan PJ (2000) Photoperiod differentially regulates the expression of Per1 and ICER in the pars tuberalis and the suprachiasmatic nucleus of the Siberian hamster. Eur J Neurosci 12:2865-2870.

Morin LP (2007) SCN organization reconsidered. J Biol Rhythms 22:3-13.

Morin LP and Allen CN (2006) The circadian visual system, 2005. Brain Res Rev 51:1-60.

Mrugala M, Zlomanczuk P, Jagota A, and Schwartz WJ (2000) Rhythmic multi-unit neural activity in slices of hamster suprachiasmatic nucleus reflect prior photoperiod. Am J Physiol 278:R987-R994.

Naito E, Watanabe T, Tei H, Yoshimura T, and Ebihara S (2008) Reorganization of the suprachiasmatic nucleus coding for day length. J Biol Rhythms 23:140-149.

Noguchi T, Watanabe K, Ogura A, and Yamaoka S (2004) The clock in the dorsal suprachiasmatic nucleus runs faster than that in the ventral. Eur J Neurosci 20:3199-3202.

Nuesslein-Hildesheim B, O'Brien JA, Ebling FJ, Maywood ES, and Hastings MH (2000) The circadian cycle of

mPER clock gene products in the suprachiasmatic nucleus of the Siberian hamster encodes both daily and seasonal time. Eur J Neurosci 12:2856-2864.

Paxinos G and Franklin KBJ (2001) *The Mouse Brain in Stereotaxic Coordinates*. 2nd ed. San Diego: Academic Press.

Pittendrigh CS and Daan SA (1976) Functional analysis of circadian pacemakers in nocturnal rodents: V. Pacemaker structure: A clock for all seasons. J Comp Physiol 106:333–355

Quintero JE, Kuhlman SJ, and McMahon DG (2003) The biological clock nucleus: A multiphasic oscillator network regulated by light. J Neurosci 23:8070-8076.

Refinetti R (2002) Compression and expansion of circadian rhythm in mice under long and short photoperiods. Integr Physiol Behav Sci 37:114-127.

Reppert SM and Weaver DR (2002) Coordination of circadian timing in mammals. Nature 418:935-941.

Rohling J, Meijer JH, VanderLeest HT, and Admiraal J (2006a) Phase differences between SCN neurons and their role in photoperiodic encoding; a simulation of ensemble patterns using recorded single unit electrical activity patterns. J Physiol Paris 100:261-270.

Rohling J, Wolters L, and Meijer JH (2006b) Simulation of day-length encoding in the SCN: From single-cell to tissue-level organization. J Biol Rhythms 21:301-313.

Schaap J, Albus H, VanderLeest HT, Eilers PH, Detari L, and Meijer JH (2003) Heterogeneity of rhythmic suprachiasmatic nucleus neurons: Implications for circadian waveform and photoperiodic encoding. Proc Natl Acad Sci U S A 100:15994-15999.

Sumová A, Bendová Z, Sládek M, Kováciková Z, and Illnerová H (2004) Seasonal molecular timekeeping within the rat circadian clock. Physiol Res 53(Suppl 1):S167-S176.

VanderLeest HT, Houben T, Michel S, Deboer T, Albus H, Vansteensel MJ, Block GD, and Meijer JH (2007) Seasonal encoding by the circadian pacemaker of the SCN. Curr Biol 17:468-473.

Vansteensel MJ, Yamazaki S, Albus H, Deboer T, Block GD, and Meijer JH (2003) Dissociation between circadian Per1 and neuronal and behavioral rhythms following a shifted environmental cycle. Curr Biol 13:1538-1542.

Yamaguchi S, Isejima H, Matsuo T, Okura R, Yagita K, Kobayashi M, and Okamura H (2003) Synchronization of cellular clocks in the suprachiasmatic nucleus. Science 302:1408-1412.